

TiO₂ Nano-doping Effect on Flux Pinning and Critical Current Density in an MgB₂ Superconductor

J.-H. Kang¹, J. S. Park², Y. P. Lee^{2*}, and V. G. Prokhorov³

¹Department of Nano and Electronic Physics, Kookmin University, Seoul 136-702, Korea

²Quantum Photonic Research Center and Department of Physics, Hanyang University, Seoul 133-791, Korea

³Institute of Metal Physics, National Academy of Sciences of Ukraine, Kiev 03142, Ukraine

(Received 24 August 2010, Received in final form 17 December 2010, Accepted 20 December 2010)

We have studied the TiO₂ doping effects on the flux pinning behavior of an MgB₂ superconductor synthesized by the *in-situ* solid-state reaction. From the field-cooled and zero-field-cooled temperature dependences of magnetization, the reversible-irreversible transition of TiO₂-doped MgB₂ was determined in the H-T diagram (the temperature dependence of upper critical magnetic field and irreversibility line). For comparison, the similar measurements are also obtained from SiC-doped MgB₂. The critical current density was estimated from the width of hysteresis loops in the framework of Bean's model at different temperatures. The obtained results manifest that nano-scale TiO₂ inclusions served as effective pinning centers and lead to the enhanced upper critical field and critical current density. It was concluded that the grain boundary pinning mechanism was realized in a TiO₂-doped MgB₂ superconductor.

Keywords : MgB₂, flux pinning, critical current density, doping

1. Introduction

The superconducting magnesium diboride (MgB₂) is of great interest due to its relatively high critical temperature, $T_c = 39$ K, which is near to liquid hydrogen with a strong coupling across the grain boundaries [1]. To be a good candidate material for practical application, it is necessary to increase the critical current density (J_c) of MgB₂ to be high enough since MgB₂ formed by conventional methods shows poor electrical connection between grains and the lack of flux pinning centers.

Generally, grain boundaries in type II superconductors can act as vortex pinning sites due to normal regions at low temperatures. Each vortex contains exactly the same flux equal to the fluxoid.

High critical currents require efficient flux pinning since J_c increases with the pinning force [2]. Therefore, grain boundaries can play important roles of pinning centers and enhance J_c . In this context, many dopants have been attempted in order to increase J_c [3, 4]. It has been shown recently that doping with SiC nano-particles enhances the J_c by formation of Mg₂Si inclusions, which

plays a role of additional effective pinning centers [5, 6]. A similar increase in the J_c can also be found with TiO₂ doping by formation of TiB₂ and MgO nano-sized impurities [7].

In our previous work, we studied the flux-pinning mechanism of grain boundaries in MgB₂ + 2 at.% TiO₂ and MgB₂ + 8 at.% SiC in terms of superconducting properties [8]. However, the behavior of the grain boundaries in MgB₂ superconductor has remained unclear.

In this work, we address a comparative study of the MgB₂ superconductor, with a dopant having a different grain size in order to elucidate grain-boundary effects on magnetic properties of MgB₂ superconductor.

2. Experimental Techniques

The samples were prepared by the *in-situ* solid-state reaction described in detail elsewhere [9]. Mechanically alloyed MgB₂ + 2 at.% TiO₂ (MBT) and MgB₂ + 8 at.% SiC (MBS) powders were used for sintering. The average grain size for the TiO₂ and SiC nano-particles was 30 and 40 nm, respectively. The microstructures of the samples were examined using high-resolution transmission-electron-microscopy (HRTEM) and electron-diffraction (ED).

*Corresponding author: Tel: +82-2-2281-5572

Fax: +82-2-2281-5573, e-mail: yplee@hanyang.ac.kr

These studies were carried out using a Philips CM 300UT-FEG microscope with a field emission gun operated at 300 kV. The resolution of the microscope was about 0.12 nm. All the micro-structural measurements were performed at room temperature. The magnetic properties measurement, such as field-cooled (FC) and zero-field cooled (ZFC) magnetization, was taken with a Quantum Design SQUID magnetometer in a temperature range of 2~40 K. The magnetization hysteresis loops [$M(H)$] were measured at an orientation of an applied magnetic field along a sample axis, which was three to four times longer than the shorter ones. The critical current density was determined indirectly from the magnetic hysteresis loop.

3. Result and Discussions

3.1. Microstructure

Microstructure plays an important role in affecting the J_c in the polycrystalline superconductor [10]. To investigate the microstructures and structural properties of the TiO₂-doped MgB₂ superconductor, TEM and ED measurements were performed. Fig. 1(a) shows the TEM image for MBT, manifesting the presence of two regions with different microstructures. The top part (A) corresponds to a coarse-grained polycrystalline structure with an average grain size of 50~70 nm, while the bottom one

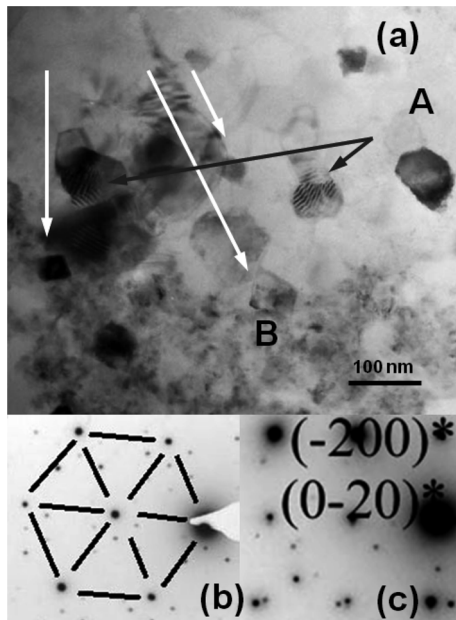


Fig. 1. (a) HRTEM image of MBT. Region A or B is coarse grain and fine grain microstructures, respectively. Black arrows indicate the moiré fringe of the stacked grains. White arrows are the MgO inclusions. (b) ED pattern for the MgB₂ and the TiB₂ grains ([0001]-zone-axis selected area). (c) ED pattern for the MgO inclusion ([001]-zone-axis selected area).

(B) exhibits the finer grained microstructure (the grain size was smaller than 10 nm). The ED pattern of the TEM image [Fig. 1(b)] reveals that both large-sized and the small-sized grains have the same hexagonal crystal lattice, which are assigned to the MgB₂ and the TiB₂ phases. The black arrows in the Fig. 1(a) are the moiré fringe of the stacked MgB₂ and TiB₂ grains. In addition, the white arrows are identified as the MgO phase, which has a cubic crystal lattice [Fig. 1(c)] The TEM analysis on the MBS sample (not shown) reveals that the MgB₂ phase has an uniform coarse-grained (the average size of the grain to be 150~200 nm) microstructure with small-sized MgO inclusions (similar to MBT).

3.2. Superconducting Properties

To probe the flux pinning state of the samples in the reversible-irreversible transition [11], temperature dependencies of the ZFC and FC magnetization were measured. Fig. 2 shows the temperature dependence of the upper critical (H_{c2}) and irreversibility (H_{irr}) fields for MBT (open symbols) and MBS (solid symbols), respectively. The $H_{c2}(T)$ was determined by the point at which the ZFC magnetization starts to deviate from the normal state linear background while the $H_{irr}(T)$ was obtained by taking the splitting point between the ZFC-FC $M(T)$ curves. The line of $H_{irr}(T)$ denoted the irreversibility line. Above and to the right of this line, the sample has a reversible magnetic behavior. Below and to the left of this line, the sample demonstrated irreversible magnetic behavior.

It can be seen from Fig. 2 that the H_{c2} of MBT was

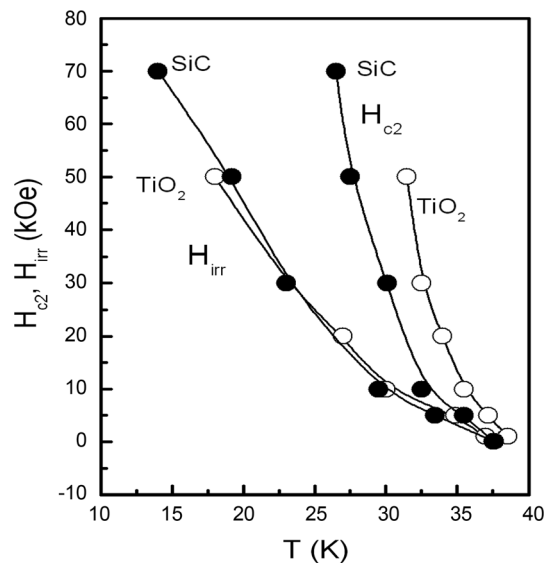


Fig. 2. Temperature dependence of the upper critical and irreversibility fields for the samples.

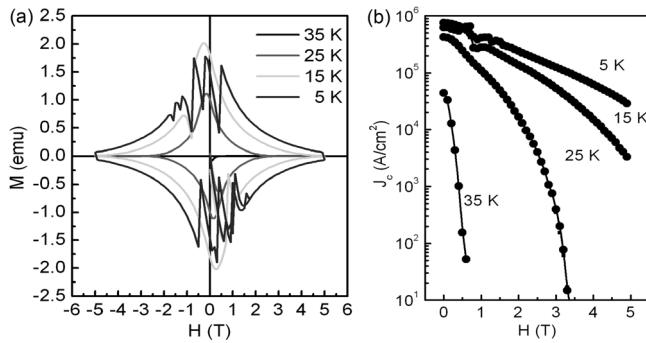


Fig. 3. (a) Hysteresis loops for MBT from 5 through 35 K. (b) Magnetic field dependence of the critical current density for MBT at various temperatures.

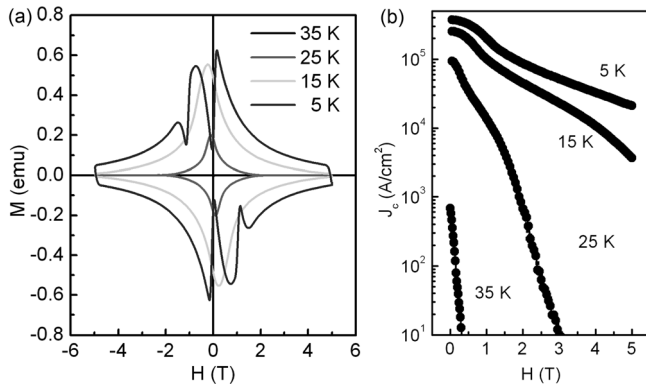


Fig. 4. (a) Hysteresis loops for MBS from 5 through 35 K. (b) Magnetic field dependence of the critical current density for MBS at various temperatures.

quite higher than that of MBS. The irreversibility field, however, is nearly coincident in both samples. Improvement of the H_{c2} for MBT is connected with formation of the fine-grained microstructure, which could lead to a decrease in the electron mean free path (and coherence length), owing to grain-boundary-electron scattering.

A magnetic J_c can be derived from the width of the magnetization loop (ΔM), being based on the Bean's model [12]:

$$J_c = \frac{20\Delta M}{a(1 - a/3b)}$$

where a , b stands for the width and the thickness of the sample, respectively.

Fig. 3(a) and 3(b) showed the magnetization loops and the field-dependent critical current densities, $J_c(H)$ of MBT at different temperatures. The similar dependencies of the MBS are presented in Fig. 4(a) and 4(b), respectively. The hysteresis loops manifest that magnetization jumps are observed in the low-field and the low-temperature range for both samples. This phenomenon is govern-

ed by the flux-jump instability of the critical state in type-II superconductors and is determined by the strong pinning and thermo-magnetic properties of the materials [13]. The hysteresis loops measured at 5 K showed larger flux-jump instability and occurred at a higher temperature (not shown) for MBT than for MBS. This can be explained by the fine-grained microstructure and the high density of the pinning centers in the MBT.

Such a suggestion is confirmed by analysis of Fig. 3(b) and 4(b). The critical current density was higher for MBT at all temperatures and applied magnetic fields, manifesting a large vortex pinning in this material.

4. Conclusions

The bulk $\text{MgB}_2 + 2 \text{ at.}\% \text{ TiO}_2$ and $\text{MgB}_2 + 8 \text{ at.}\% \text{ SiC}$ were prepared using the *in-situ* solid-state reaction. A HRTEM study revealed that the TiO_2 -doped MgB_2 had a finer grained microstructure than that of SiC-doped one. The decrease in grain size of the dopant owing to nanodoping leads to an enhanced upper critical field and critical current density. We conclude that the TiO_2 nanoparticle is a more effective flux pinning center due to the grain-boundary effect.

Acknowledgement

This work was supported by the Korea Science and Engineering Foundation (KOSEF) through the Quantum Photonic Science Research Center and by the Ministry of Education, Science and Technology (MEST), Korea; this work was also supported by research program 2008 of Kookmin University in Korea (J.-H. Kang).

References

- [1] J. Nagamatsu, N. Nakagawa, T. Muranaka, Y. Zenitani, and J. Akimitsu, *Nature* **410**, 63 (2001).
- [2] C. Giovannella, G. Collin, P. Rouault, and I. A. Campbell, *Europhys. Lett.* **4**, 109 (1987).
- [3] X. Z. Liao, A. Serquis, Y. T. Zhu, J. Y. Huang, L. Civale, D. E. Peterson, F. M. Mueller, and H. F. Xu, *J. Appl. Phys.* **93**, 6208 (2003).
- [4] S. H. Zhou, A. V. Pan, M. J. Qin, H. K. Lin, and S. X. Dou, *Physica C* **387**, 321 (2003).
- [5] S. X. Dou, S. Soltanian, J. Horvat, X. L. Wang, S. H. Zhou, M. Ionescu, H. K. Liu, P. Munroe, and M. Tomsic, *Appl. Phys. Lett.* **81**, 3419 (2002).
- [6] Q. W. Yao, X. L. Wang, J. Horvat, and S. X. Dou, *Physica C* **402**, 38 (2004).
- [7] Y. Zhao, Y. Feng, T. Machi, C. H. Cheng, D. X. Huang, Y. Fudamoto, N. Koshizuka, and M. Murakami, *Europhys.*

- Lett. **57**, 437 (2002).
- [8] V. G. Prokhorov, G. G. Kaminsky, V. L. Svetchnikov, J. S. Park, T. W. Eom, Y. P. Lee, J.-H. Kang, V. A. Khokhlov, and P. Mihkeenko, *Low Temperature Physics* **35**, 439 (2009).
- [9] E. Martínez, P. Mikheenko, M. Martínez-López, A. Millán, A. Bevan, and J. S. Abell, *Phys. Rev. B* **75**, 134515 (2007).
- [10] D. C. Larbalestier, M. Daeumling, X. Cai, J. Seuntjens, J. McKinnell, D. Hampshire, P. Lee, C. Meingast, T. Willis, H. Muller, R. D. Ray, R. G. Dillenburg, E. E. Hellstrom, and R. Joynt, *J. Appl. Phys.* **62**, 3308 (1987).
- [11] R. H. Koch, V. Foglietti, W. J. Gallagher, G. Koren, A. Gupta, and M. P. A. Fisher, *Phys. Rev. Lett.* **63**, 1511 (1989).
- [12] C. P. Bean, *Rev. Mod. Phys.* **36**, 31 (1964).
- [13] Y. Kimishima, S. Takami, T. Okuda, M. Uehara, T. Kuramoto, and Y. Sugiyama, *Physica C* **463-465**, 281 (2007).